Published in final edited form as:
J Neurosci. 2008 November 19; 28(47): 12510–12522. doi:10.1523/JNEUROSCI.4329-08.2008.

scn1bb, a zebrafish ortholog of *SCN1B* expressed in excitable and non-excitable cells, affects motor neuron axon morphology and touch sensitivity

Amanda J. Fein[1,¶], **Melissa A. Wright**[2,3,¶], **Emily A. Slat**[1,4], **Angeles B. Ribera**[2], and **Lori L. Isom**[*,1]

[1]Department of Pharmacology, University of Michigan, 1301 MSRB III, 1150 W. Medical Center Dr., Ann Arbor, MI 48109-0632, Tel (734) 936-3050, Fax (734) 763-4450

[2]Department of Physiology and Biophysics□, University Colorado Denver at Anschutz Medical Campus□(UCD at AMC), RC-1 North Tower, P18-7117, PO Box 6511, Mail Stop F8307, Aurora, CO 80045-6511, Tel (303) 724-4517; Fax (303) 724-4501

[3]Medical Scientist Training Program□, University Colorado Denver at Anschutz Medical Campus□ (UCD at AMC), RC-1 North Tower, P18-7117, PO Box 6511, Mail Stop F8307, Aurora, CO 80045-6511, Tel (303) 724-4517; Fax (303) 724-4501

Abstract

Voltage-gated Na^+ channels initiate and propagate action potentials in excitable cells. Mammalian Na^+ channels are composed of one pore-forming α subunit and two β subunits. *SCN1B* encodes the Na^+ channel β1 subunit that modulates channel gating and voltage-dependence, regulates channel cell surface expression, and functions as a cell adhesion molecule (CAM). We recently identified *scn1ba*, a zebrafish ortholog of *SCN1B*. Here we report that zebrafish express a second β1-like paralog, *scn1bb*. In contrast to the restricted expression of *scn1ba* mRNA in excitable cells, we detected *scn1bb* transcripts and protein in several ectodermal derivatives including neurons, glia, the lateral line, peripheral sensory structures, and tissues derived from other germ layers such as the pronephros. As expected for β1 subunits, elimination of Scn1bb protein *in vivo* by morpholino knock-down reduced Na^+ current amplitudes in Rohon-Beard neurons of zebrafish embryos, consistent with effects observed in heterologous systems. Further, after Scn1bb knock-down, zebrafish embryos displayed defects in Rohon-Beard mediated touch sensitivity, demonstrating the significance of Scn1bb modulation of Na^+ current to organismal behavior. In addition to effects associated with Na^+ current modulation, Scn1bb knockdown produced phenotypes consistent with CAM functions. In particular, morpholino knock-down led to abnormal development of ventrally-projecting spinal neuron axons, defasciculation of the olfactory nerve, and increased hair cell number in the inner ear. We propose that, in addition to modulation of electrical excitability, Scn1bb plays critical developmental roles by functioning as a CAM in the zebrafish embryonic nervous system.

Keywords

Na^+ channel; auxiliary subunit; cell adhesion; electrophysiology; zebrafish; touch-sensitivity

[¶]These authors contributed equally to the work and are considered to be co-first authors.
[4]Present address: Medical Scientist Training Program, Washington University School of Medicine, St. Louis, MO 63110
[*]Corresponding author, email: lisom@umich.edu

Introduction

In addition to well-known ion conduction roles, voltage-gated channels regulate processes as diverse as transcriptional regulation, protein scaffolding, cell adhesion, and intracellular signaling (Dolmetsch, 2003; MacLean et al., 2003; MacLean et al., 2005; Gomez-Ospina et al., 2006; Hegle et al., 2006; Kaczmarek, 2006; Levitan, 2006; Kim et al., 2007; Brackenbury et al., 2008a; Brackenbury and Isom, 2008). In some cases, the latter non-traditional roles of ion channels can occur even in the absence of ion flux. Thus, voltage-gated ion channels have the potential to regulate intercellular and intracellular signaling, and *vice versa*.

Voltage-gated Na^+ channels are traditionally considered to be responsible for initiating and propagating action potentials in excitable cells (Catterall, 2000). Neuronal Na^+ channels comprise a central, ion-conducting α subunit and two β subunits. While not part of the ion-conducting pore, β subunits modulate ion channel gating and voltage-dependence and regulate Na^+ channel cell surface expression. Moreover, β subunits possess immunoglobulin superfamily motifs (Isom and Catterall, 1996) and can function as cell adhesion molecules (CAMs), both in the presence and absence of the ion-conducting pore (Isom, 2001). Thus, β subunits extend the functional capabilities of Na^+ channels beyond ion flux.

In vitro, homophilic interactions of β1 or β2 result in cellular aggregation and ankyrin recruitment (Malhotra et al., 2000; Malhotra et al., 2002). β1 homophilic cell adhesion promotes neurite extension *in vitro* (Davis et al., 2004) and *Scn1b* null mice show defective axon extension and fasciculation *in vivo* (Brackenbury et al., 2008c). Interactions of β1 or β2 with the extracellular matrix molecule tenascin-R influence cell migration (Srinivasan et al., 1998; Xiao et al., 1999). β1 interacts heterophilically with several other CAMs, including contactin, NrCAM, neurofascin, cadherin, and connexin (Kazarinova-Noyes et al., 2001; Malhotra et al., 2004; McEwen and Isom, 2004; McEwen et al., 2004; Brackenbury et al., 2008c; Brackenbury and Isom, 2008). *In vivo*, formation and/or stability of Na^+ channel signaling complexes at nodes of Ranvier require heterophilic association of β1 with contactin (Chen et al., 2004) and β1-mediated neurite outgrowth requires both contactin and fyn kinase (Brackenbury et al., 2008c). β subunits also serve as substrates for γ-secretase and BACE1 in primary neurons, suggesting roles in neuronal development and/or pathophysiology (Kim et al., 2005; Wong et al., 2005; Kim et al., 2007).

We recently cloned the zebrafish gene, *scn1ba*, encoding a β1 subunit that is expressed as two splice variants, *scn1ba_tv1* and *scn1ba_tv2*, but only in excitable cells (Fein et al., 2007). In contrast, expression of the mammalian *SCN1B* occurs in both traditionally “non-excitable” tissues as well as excitable cells (Oh and Waxman, 1994a, 1995; Diss et al., 2004). On this basis, we hypothesized that zebrafish might express additional *SCN1B* orthologs. Here, we report the identification of a second β1-like paralog, *scn1bb*, that is not only expressed in excitable tissues but also in the optic nerve myelin sheath, Schwann cells, radial glia, lateral line primordia and neuromasts, olfactory and otic epithelia, and the pronephric duct epithelium. The combined expression patterns of *scn1ba* and *scn1bb* resemble that of mammalian *SCN1B*, consistent with subfunctional partitioning in teleost duplicated genes. Moreover, morpholino knock-down of Scn1bb protein produces defects consistent with misregulation of Na^+ current and cell adhesion, revealing both traditional and non-traditional roles for Na^+ channel β1 subunits in the developing zebrafish nervous system.

Materials and Methods

Animals

Adult zebrafish (*D. rerio*) were maintained at the University of Michigan School of Medicine or in the Center for Comparative Medicine at University of Colorado Denver at 28.5°C and

bred according to established procedures (Westerfield, 1995). Animal protocols were approved by the University of Michigan and the University of Colorado Committees on Use and Care of Animals. The transgenic zebrafish line Tg(Hb9:GFP) was obtained from M. Fox and J. Sanes at Harvard University ((Flanagan-Steet et al., 2005).

Cloning

scn1bb was identified by performing a Blast search for zebrafish sequences with significant homology to the rat *Scn1b* peptide sequence (GenBank AAH94523) (Isom et al., 1992) *scn1bb* was identified in the EST pool (GenBank EF394326) and the full length clone was purchased from Open Biosystems (Huntsville, AL). The clone was provided in the pME18S-FL3 vector. The cDNA insert was amplified by polymerase chain reaction using oligonucleotides developed to the pME18S-FL3 vector (5′-CTAGCGGCCGCGACCTGC-3′ and 5′-TCATTTTATGTTTCAGGT-3′, forward and reverse, respectively) and ligated into the pGEM-T Easy vector (Promega, Madison, WI). *scn1bb* was subsequently excised with Not I and subcloned into the SP64T-BXN vector (Isom et al., 1992) for electrophysiological recording. Construction of a *scn8aa* vector for oocyte expression was described previously (Fein et al., 2007).

Mapping

scn1bb was mapped using the LN54 radiation hybrid panel (Marc Ekker, Loeb Institute). PCR was performed using DNA from each of the 93 cell lines or control DNA as template using *scn1bb* forward (5′-ATGGCTCTGAGAACATCATCG-3′) and reverse (5′-GTGCACGTCTTTACTGGTGACCTT-3′) oligonucleotides. This reaction resulted in the amplification of a 245 bp product corresponding to *scn1bb*. PCR products were analyzed on agarose gels to determine which cell lines were positive for *scn1bb*. Each cell line was scored and the results entered into the LN54 mapping website **(**http://mgchd1.nichd.nih.gov:8000/zfrh/beta.cgi) which statistically determined the linkage group (LG) for *scn1bb*.

Antibody and toxin labels

Monoclonal anti-α-acetylated tubulin and anti-pan-Na^+ channel antibodies were obtained from Sigma (St Louis, MO). Polyclonal anti-claudin b was obtained from Dr. A.J. Hudspeth, Rockefeller University. The zn-8 and zrf-1 mouse monoclonals were developed by Dr. B. Trevarrow (Fashena and Westerfield, 1999) and was obtained from the Developmental Studies Hybridoma Bank developed under the auspices of the NICHD and maintained by the University of Iowa, Department of Biological Sciences, Iowa City, IA 52242. Oregon-Green conjugated phalloidin, Alexa 488 conjugated anti-rabbit IgG and Alexa 594 conjugated anti-mouse IgG were obtained from Molecular Probes (Carlsbad, CA).

An affinity-purified polyclonal antibody to Scn1bb was generated by Open Biosystems (Hunstville, AL) as fee-for-service. The peptide sequence of the epitope was: EHYEFSKVTSKD. Anti-Scn1bb was characterized by Western blot and by immunostaining. Specificity was demonstrated by recognition on Western blots of recombinant Scn1bb protein expressed in transfected cells (Supplemental Fig. 1 A, B). cDNAs encoding *scn1bb* or *scn1ba* (Fein et al., 2007) were subcloned in the pcDNA3.1-Hygro vector (Invitrogen, Carlsbad, CA) and used to transiently transfect Chinese hamster lung 1610 cells (Isom et al., 1995). Cells grown to 80% confluence in 100 mm dishes were transfected with 8 μg DNA using Fugene 6 reagent (Roche, Indianapolis, IN) according to the manufacturer's instructions and harvested 48 hours post-transfection. Mouse brain, rat brain, and zebrafish membranes (from whole fish) were prepared as described (McEwen et al., 2004). Equal aliquots of each protein sample were resuspended in SDS-PAGE sample buffer containing 1% SDS and 500 mM β-mercaptoethanol and heated to 70°C for 5 min. Samples were separated on 10%

polyacrylamide SDS-PAGE gels and transferred to nitrocellulose. The Western blot was probed with anti-Scn1bb at a dilution of 1:500 followed by goat anti-rabbit secondary antibody conjugated to HRP (1:2,000). Chemiluminescent signals were detected with West Femto reagent (Pierce, Rockford, IL).

Anti-Scn1bb antibody specificity was further determined by blocking the antibody before performing immunohistochemistry with an equivalent volume of immunizing peptide at a concentration of 1 mg/ml for 1 h at room temperature. This manipulation abolished the immune signal (Supplemental Fig. 1C). Anti-acetylated α-tubulin antibody was used as a pan-neuronal marker in this experiment. Anti-Scn1bb or anti-acetylated α-tubulin signals were detected using Alexa 488 conjugated anti-rabbit IgG secondary antibody or Alexa 594 conjugated anti-mouse IgG secondary antibody, respectively.

Immunocytochemistry

Immunocytochemistry was performed on whole mount embryos as described (Woods et al., 2006) or on dissected adult optic nerves as described (Voas et al., 2007). Whole fish were fixed in 4% paraformaldehyde for 30 min; dissected nerves were fixed for 10 min. Embryos were then washed in standard phosphate buffered saline containing 0.8% Triton X-100 (PBT), water, and acetone and then blocked in PBT containing 10% goat serum. Dissected nerves were washed in PBT and then placed directly in the PBT blocking solution containing 10% goat serum. Anti-Scn1bb (1:500), anti-acetylated α-tubulin (1:1000), pan Na^+ channel (1:500), anti-claudin b (1:250), zn-8 (1:200), or zrf-1 (1:10) antibodies diluted in PBT containing 10% goat serum, were applied overnight at 4°C to either preparation. Phalloidin (Molecular Probes-Invitrogen) was used at a concentration of 1:40. The following day the embryos and nerves were washed with PBT, and secondary antibody diluted in PBT with 10% goat serum, was applied. Anti-Scn1bb antibody signal was detected using Alexa 488 conjugated anti-rabbit IgG. Zn-8, anti-acetylated α-tubulin, or pan-Na^+ channel antibodies were detected using Alexa 594 conjugated anti-mouse IgG. Embryos and nerves were then washed with PBT and mounted for viewing with an Olympus FluoView 500 confocal microscope located in the University of Michigan Department of Pharmacology. Images were collected with FluoView 4.3 software and analyzed with Adobe Photoshop.

Fish were also cryosectioned (10 μm) and stained following standard methods (Chen et al., 2004). Briefly, fish were fixed for 1 h at room temperature in 4% paraformaldehyde. They were placed in 30% sucrose and stored overnight at 4°C. Fish were then mounted in optimal cutting temperature compound (OCT) on dry ice and stored at -80°C until slicing. Once sectioned, samples were blocked with phosphate buffer (0.02 M NaH_2PO_4, 0.08 M Na_2HPO_4) containing 0.3% Triton X-100 and 10% normal goat serum. Sections were incubated overnight with anti-Scn1bb antibody (1:500) and anti-acetylated α-tubulin antibody (1:2000) at room temperature. Anti-Scn1bb antibody signal was detected using Alexa 488 conjugated anti-rabbit IgG, and anti-acetylated α-tubulin was detected using Alexa 594 conjugated anti-mouse IgG. Images were collected with a Zeiss Axiophot-2 fluorescent microscope equipped with a Zeiss Axiocam CCD digital camera and Axio Vision software, located in the University of Michigan Microscopy and Image Analysis Laboratory and analyzed with Adobe Photoshop. High magnification images were obtained and analyzed using an Olympus FluoView 500 confocal microscope, FluoView 4.3 software, and Adobe Photoshop.

Electrophysiology

Whole-cell recordings from Rohon-Beard (RB) neurons were obtained *in situ* as described previously (Ribera and Nüsslein-Volhard, 1998; Pineda et al., 2005). Briefly, 48 hpf embryos were sacrificed in the presence of tricaine and then mounted dorsal side up onto a glass slide.

The skin and meninges surrounding the spinal cord were removed. Whole cell patch clamp methods were then used to record Na^+ currents.

Morpholino Injections

Morpholino antisense oligonucleotides (MOs) were synthesized by Gene Tools (Philomath, Oregon). The Scn1bb MO (Scn1bbMO1) targeted the predicted translation start methionine of *scn1bb* and had 25 residues with the following sequence: 5′ AGGTGCCGCACACACTCCTGCATGG-3′. A control MO (Scn1bbCTL), with an inverse sequence was also synthesized (5′GGTACGTCCTCACACACGCCGTGGA-3′). Scn1bbCTL injected embryos served as controls. A second translation blocking MO (5′ CGAATGGACGGACAGACGAGCACTC-3′), Scn1bbMO2, was also synthesized and yielded similar results to Scn1bbMO1. For simplicity, both translation blocking MOs will be referred to as Scn1bbMO. MOs were injected into the yolk at 1- to 2-cell at concentrations ranging between 2.5-4 ng/nl in 1% Fast Green.

Touch sensitivity

To prioritize testing of sensory rather than motor function, we limited our tests of touch insensitivity to embryos that could swim spontaneously with a normal pattern (Pineda et al., 2005). In brief, with a metal probe, we gently touched the dorsal trunk of the embryo. We waited ~3 seconds and reapplied the probe for a total of ten trials. Responses were scored as follows: 0, no response; 0.5, non-swimming response (e.g., segmentally restricted trunk bend); 1.0, normal swimming response. The scores of each of the ten trials were summed to yield final touch response scores between 0 and 10.

Confocal imaging of morphant phenotypes

Three different phenotypes were analyzed in detail on a Zeiss LSM5 Pascal Confocal Microscope: motor axon morphology, hair cell number, and olfactory nerve branching in the olfactory bulb. To analyze motor axon branching, live 72 hpf Tg(Hb9:GFP) embryos injected with either Scn1bbMO or Scn1bbCTL were mounted laterally between two coverslips in 0.5% Low Melting Point Agarose dissolved in Embryo Media with Tricaine. Images were collected as z-stacks and projected for analysis. Approximately 600 μm of the trunk was imaged in overlapping z-stacks for each embryo, starting with the third segment. Overlapping projected stacks were aligned using Photoshop. Axon branches were traced in Photoshop and counted for each embryo. To measure the (1) number of branches of the olfactory nerve or (2) the number of hair cells in the otic vesicle, embryos were stained for either acetylated α-tubulin or actin (using Phalloidin), respectively. Labeled embryos were laterally mounted in 1% agarose. Images of the olfactory nerve or otic vesicle, respectively, were collected as z-stacks using a 40x objective. The outline of the olfactory nerve was traced in Photoshop and the number of branches within the olfactory pit was counted. Phalloidin-stained hair cell bundles were counted from projected stacks.

Results

Zebrafish scn1bb is homologous to Scn1b and scn1ba

We identified a second *SCN1B* ortholog in zebrafish, *scn1bb* (according to the zebrafish nomenclature convention: http://zfin.org/zf_info/nomen.html) that encodes the protein Scn1bb. Alignment of zebrafish Scn1bb with rat Scn1b shows that the two β1 subunit proteins share 51% amino acid identity (Fig. 1, residues in red), with an additional 16% of residues that are strongly similar, and 11% of residues that have weak similarity. The previously isolated zebrafish β1-like ortholog, *scn1ba*, predicts a protein that shares 65% identity with Scn1bb (Fig. 1, residues in green; (Chopra et al., 2007; Fein et al., 2007)).

The Scn1bb sequence contains an N-terminal signal peptide followed by the start of the mature protein at residue A-25 (Fig. 1, signal peptides underlined in blue) corresponding to the experimentally confirmed site in Scn1b (Isom et al., 1992). The amino acid sequences of the three zebrafish β1-like subunits predict a single transmembrane domain (Fig. 1, boxed residues). Similar to Scn1ba (Fein et al., 2007), Scn1bb contains two conserved cysteine residues that are predicted to form an extracellular Ig loop domain (Fig. 1, cysteines in blue and underlined) (McCormick et al., 1998). Examination of the predicted β sheets of the extracellular Ig loop domain reveals that the residues that lie along the A/A' face, a known site of interaction with the α subunit in mammals, are highly conserved in the zebrafish β1 paralogs (McCormick et al., 1998).

Similar to Scn1ba, Scn1bb contains a conserved tyrosine at position 180 (Fig. 1, yellow highlight) that corresponds to tyrosine-181 in Scn1b. This tyrosine has been shown to be important for recruitment of ankyrin, Scn1b sub-cellular localization, and Scn1b-mediated channel modulation *in vitro* (Malhotra et al., 2002; Malhotra et al., 2004). In contrast to the 4 predicted N-linked glycosylation sites in mammalian Scn1b or zebrafish Scn1ba, Scn1bb contains only two N-linked glycosylation sites (Fig. 1, N-90 and N-94, arrowheads; NetNGlyc 1.0 - http://www.cbs.dtu.dk), a feature that may result in different effects of each Scn1b paralog on modulation of gating of various Na^+ channel α subunits (Johnson et al., 2004).

Map position of scn1bb

Identification of the *scn1bb* gene in combination with the previous isolation of *scn1ba* reveals that zebrafish has two genes that are orthologous to the single mammalian *SCNB1* gene. Zebrafish s*cn1bb* and the previously identified *scn1ba* show high sequence similarity, as expected for duplicated genes. Duplicated genes can arise in tandem and reside near each other. Alternatively, duplicated genes, especially in teleosts, can arise by large scale genome duplication. To determine the origins of the multiple *SCNB1* orthologs in zebrafish, we first determined whether *scn1bb* resides near *scn1ba*, as expected for tandem duplication events, or on another linkage group (LG), consistent with large scale genome duplication. We mapped the position of scn1bb to LG19. The best overall marker linked to *scn1bb* was Z4379 with a logarithm of the odds (lod) score of 20.1, positioning *scn1bb* 2.84 cR from Z4379 (http://mgchd1.nichd.nih.gov:8000/zfrh/beta.cgi). In contrast, *scn1ba* mapped to LG16 (Fein et al., 2007). Interestingly, LG16 and LG19 have been shown to be a duplicate chromosomal pair, based on analysis of the gene content of these two chromosomes (Woods et al., 2005), supporting the possibility that *scn1ba* and *scn1bb* are duplicates arising from a genome-wide duplication event.

If *scn1ba* and *scn1bb* were duplicates, we would expect these genes to be orthologous to and show synteny with the same mammalian gene (*Scn1b*). A high degree of synteny exists between *scn1ba* and mouse *Scn1b* (Fein et al., 2007). We did not observe synteny between *scn1bb* and *Scn1b*. However, chromosomal rearrangements occur during evolution that can obscure the original syntenic relationships between genes (Postlethwait, 2006). On this basis, we named the new β1-like subunit gene *scn1bb* to reflect its high similarity to its presumed duplicate, *scn1ba*.

Scn1bb protein expression in central and peripheral glia

We previously reported expression of *scn1ba*, the gene duplicate of *scn1bb*, throughout the retina and optic nerve (Fein et al., 2007). On this basis, we determined the localization of Scn1bb in the retina and optic nerve at 5 dpf in 10 μm cryo-sections. In contrast to Scn1ba, we observed no retinal expression of Scn1bb. Interestingly, the only significant anti-Scn1bb staining in this region appeared in cells that surrounded the optic nerve (Fig. 2 A-C). As expected, anti-acetylated α-tubulin strongly labeled optic nerve axons and some retinal layers

but not cells surrounding the optic nerve (Fig. 2 B, ON) (Fein et al., 2007). The merged image showed no overlap between the expression patterns of the two proteins (Fig. 2 C).

We next compared the localization of Scn1bb to that of voltage-gated Na^+ channels in isolated optic nerves. Na^+ channels localize in high density clusters at nodes of Ranvier in central and peripheral myelinated axons in mammals (Girault and Peles, 2002; Kazarinova-Noyes and Shrager, 2002) and have been detected in the zebrafish posterior lateral line (PLL) nerve (Woods et al., 2006). In isolated adult optic nerve preparations, we observed anti-Scn1bb labeled cells wrapping the optic nerve axons (Fig. 2 D, F). In contrast, pan-Na^+ channel α-subunit antibody labeled optic nerve axons on which high density clusters (arrowheads), possibly developing hemi-nodes, were evident (Fig. 2 E, F). In the merged image, Scn1bb immunoreactivity was limited to the myelinating glial processes in the optic nerve and was absent from the axons (Fig. 2 F). Importantly, Na^+ channel α-subunit immunoreactivity was absent from the oligodendrocyte processes wrapping the axons, suggesting that Scn1bb is expressed independently of the α-subunit and plays a non-conducting role in the myelin sheath.

We also observed expression of Scn1bb in the spinal cord of 72 hpf larvae. Anti-Scn1bb labeled a network of cells with parallel processes at regular intervals (Fig. 2 G). These Scn1bb positive cells were negative for two different neuronal markers, zn8 and α-tubulin staining (Fig. 2G and data not shown) (Fashena and Westerfield, 1999). The Scn1bb immunopositive cells extended long radial processes dorsally, as previously described for radial glia (Fig. 2 G) (Lewis and Eisen, 2003). In addition, peripheral Schwann cells showed Scn1bb immunoreactivity (Fig. 2 H, I, arrows). The identification of the Scn1bb immunopositive cells in the periphery as Schwann cells was made on the basis of their location surrounding peripheral motor nerves (Fig. 2 H, I) and positive immunoreactivity for zrf-1, an antibody that recognizes the glial marker, glial fibrillary associated protein (Fig. 2 I). Interestingly, not all of the Scn1bb signal in Fig. 2 I is positive for zrf-1, raising the possibility that Scn1bb may be expressed in other cells that ensheath motor nerves, e.g. perineurial glia (Kucenas et al., 2008).

Scn1bb protein localizes to lateral line structures

The lateral line system in zebrafish mediates behaviors involved in predator avoidance and courtship. The lateral line system consists of nerves and external mechanosensory organs, called neuromasts, that are responsive to changes in water movement (Whitfield, 2005). Several characteristics of the lateral line made it an attractive system to investigate with respect to Scn1bb. First, the lateral line system consists of both excitable as well as non-excitable cells. Second, the development of the lateral line system requires interactions among the different cell types, a process that likely involves CAM function.

We first determined whether Scn1bb was expressed early during lateral line development. During formation of the lateral line in the trunk (PLL), neuromasts are deposited by migration of two different primordia, known as prim I and prim II. Prim I migration occurs between 20 - 42 hpf. As prim I migrates posteriorly, it deposits discrete groups of cells, proneuromasts, along the horizontal myoseptum across the full length of the trunk. Sensory axons of the octavolateralis system closely follow this migration (Sapede et al., 2002; Lopez-Schier et al., 2004). We detected Scn1bb immunoreactivity in prim I in 28 hpf embryos, during early stages of the migration process (Fig. 3 A). At this time, prim I did not express the neural marker, acetylated α-tubulin, but the trailing axon did (Fig. 3 A, long arrow).

At relatively much later stages (3-7 dpf), prim II migrates posteriorly and deposits the secondary neuromasts, thus forming the remainder of the mature posterior lateral line (Sapede et al., 2002). At 5 dpf, prim II expressed Scn1bb (Fig. 3 B). In addition, Scn1bb localized to newly deposited neuromasts trailing the primordium (Fig. 3B, arrowheads). At this early stage, the neuromasts were not yet labeled by anti-acetylated α-tubulin, although innervating neurites

were labeled (Fig. 3 B, long arrow). In contrast, claudin b is expressed in migrating primordial cells similar to Scn1bb (Lopez-Schier et al., 2004). We observed no overlap between anti-claudin b labeling in prim II and the trailing neurites labeled by anti-acetylated α-tubulin (Fig 3 C). These results indicate that Scn1bb is present during the early stages of PLL migration similar to claudin b.

In addition to the PLL, zebrafish also have an anterior lateral line system. At 5 dpf, anti-Scn1bb labeled each neuromast in the anterior lateral line (Fig. 3 D, arrowheads). PLL neuromasts were similarly labeled at this stage (Fig. 3 E). In neuromasts, anti-acetylated α-tubulin identifies hair cell somata as well as the kinocilia projecting from the neuromast hair cell bundle (Raible and Kruse, 2000; Lopez-Schier et al., 2004). Although acetylated α-tubulin and Scn1bb expression were detected in the same neuromast (Fig. 3 D-F), the two expression patterns were non-overlapping. Rather than labeling the kinocilia of the hair cells, as did anti-acetylated α-tubulin, anti-Scn1bb labeled the supporting cells found at the base of the neuromast (Fig. 3 F).

Scn1bb protein expression in the olfactory system

Similar to the lateral line, the zebrafish olfactory system develops early and consists of many different cell types (Hansen and Zeiske, 1993). We observed expression of Scn1bb in the olfactory pits at 5 dpf in addition to lateral line neuromasts (Fig. 4 A; OP indicates olfactory pits; arrowheads indicate neuromasts). Anti-acetylated α-tubulin labeled cilia projecting from olfactory sensory neurons (OSNs) as well as the kinocilia of the intervening supporting cells, as shown previously (Tsujikawa and Malicki, 2004). Glia-like olfactory supporting cells, also called sustentacular cells (Hegg and Lucero, 2006), are arranged in a ring at the rim of the olfactory pit, interspersed with ciliated OSN dendritic knobs, resulting in a dense fringe of acetylated α-tubulin-positive cilia (Fig. 4 B) (Hansen and Zeiske, 1993). Merging of these two images showed that Scn1bb and acetylated α-tubulin do not colocalize and that expression of Scn1bb is limited to the supporting cells (Fig. 4 C).

At higher magnification, Scn1bb protein was evident in the supporting cell somata but absent from the cilia and the OSN dendritic knobs (Fig. 4 D). In contrast, anti-acetylated α-tubulin showed strong labeling of the outward projecting cilia and weak labeling in the OSN dendritic knobs (Fig. 4 E, arrows). In the merged image, expression of Scn1bb was observed interspersed between the OSN dendritic knobs, in close apposition to, but not overlapping with, the expression domain of acetylated α-tubulin (Fig. 4 F).

Non-neuronal cells of the inner ear cells also express Scn1bb protein

The zebrafish inner ear sensory system develops early, has multiple cell types and shares structural and functional similarity with the lateral line (Nicolson, 2005). At 5 dpf, we detected Scn1bb immunoreactivity in the epithelial pillars (ep) around which the semi-circular canals form (Fig. 5 A). This was in contrast to the expression of acetylated α-tubulin in the kinocilia of the surrounding sensory regions including the anterior macula (am), posterior macula (pm) and posterior cristae (pc) (Fig. 5 B). Merging the two staining patterns revealed non-overlapping expression of Scn1bb and acetylated α-tubulin in inner ear (Fig. 5 C). In addition to the epithelial pillars of the inner ear, anti-Scn1bb also labeled the supporting cells at the base of one of the otic neuromasts (Fig. 5 D arrowhead) (Raible and Kruse, 2000). In agreement with our previous findings (Fig. 3), acetylated α-tubulin labeled the kinocilia projecting from the center of the neuromast (Fig. 5 E arrowhead), and its expression was non-overlapping with Scn1bb (Fig. 5 F). Scn1bb immunoreactivity did not overlap with another neuronal marker, zn-8 (Fig. 5 G-I). Taken together, the data indicate that Scn1bb localizes to non-neuronal cells in neuromasts of the inner ear.

Scn1bb protein localizes to epithelia in the developing kidney

In light of Scn1bb's expression pattern in non-neuronal ciliated cells within sensory structures, we tested whether Scn1bb was expressed in other non-neuronal ciliated cells. Our initial *in situ* hybridization studies (Supplemental Fig. 2) revealed *scn1bb* mRNA in the embryonic kidney, or pronephros, an organ composed of ciliated cells. Similar to lateral line neuromasts, the pronephric ducts form from tissue deposits laid by migrating primordia (Drummond et al., 1998). The ducts comprise polarized epithelial cells that are lined with cilia. Formation of the ducts is completed by 24 hpf (Drummond, 2003; Drummond, 2005). At 28 hpf, the pronephros contained Scn1bb protein within the duct (Fig. 6 A, arrow). Anti-acetylated α-tubulin labeled the cilia lining the length of the ducts, as demonstrated previously (Fig. 6 B) (Drummond, 2005). When we examined the pronephric duct at higher magnification at the point where the duct reaches the cloaca, we observed that anti-Scn1bb labeled the epithelial cells that line the duct (Fig. 6 D), whereas anti-acetylated α-tubulin labeled the ciliated interior of the duct (Fig. 6 E). As in the lateral line and inner ear, expression of the two proteins was non-overlapping (Fig. 6 F). At even higher magnification, it was evident that Scn1bb is ubiquitously present in the epithelial cells (Fig. 6 G), whereas acetylated α-tubulin is expressed in the cilia projecting from these cells (Fig. 6 H). The expression patterns of the two proteins are in close apposition, but non-overlapping in the pronephros (Fig. 6 I).

Scn1bb modulates neuronal function in vivo

To identify *in vivo* roles of Scn1bb in nervous system function and development, we used a morpholino-based approach to knock-down Scn1bb. We injected embryos with either a translation blocking morpholino targeting Scn1bb (Scn1bbMO) or a control morpholino (Scn1bbCTL). We first tested for roles in ion conduction, as expected for a subunit of voltage-gated sodium channel complexes. Similar to mammalian Scn1b, Scn1bb modulates the tetrodotoxin-sensitive Na^+ channel α subunit scn8aa (encoding nav1.6a) when co-expressed in a heterologous system (Supplemental Fig. 3 and Supplemental Tables 1 and 2). Whereas our survey of Scn1bb protein expression focused on non-neuronal cell types, we had also detected scn1bb mRNA in RB neurons (Supplemental Fig. 2).

Accordingly, we first tested for *in vivo* effects on native currents. We recorded Na^+ currents in RB neurons, because these cells express both *scn8aa* and *scn1bb* mRNAs and are accessible to whole-cell recording methods (Ribera and Nüsslein-Volhard, 1998). RB neurons serve as primary mechanosensory neurons for the developing embryo before dorsal root ganglia develop (Clarke et al., 1984). In contrast to the dorsal root ganglia, RB somata reside within the central nervous system in the dorsal most aspect of the spinal cord. We found that Na^+ current peak amplitudes were significantly reduced in Scn1bb morphants compared to controls, consistent with effects observed for heterologously expressed subunits (Fig. 7 A; Supplemental Figure 3).

The decrease in RB Na^+ current amplitudes produced by Scn1bb knock-down raised the possibility that the behavior mediated by RB neurons, the touch response, would be defective in morphant embryos. We found that injection of the Scn1bb MO, but not the control MO, led to a significant reduction in touch sensitivity (Fig. 7 B). These *in vivo* findings indicate that voltage-gated Na^+ channel function *in vivo* shows an essential requirement for Scn1bb.

Knock-down of Scn1bb produces phenotypes associated with defective CAM function

We examined Scn1bb morphant embryos for phenotypes that have previously been found when either Na^+ channel α or β subunits have been eliminated during developmental stages (Pineda et al., 2006; Brackenbury et al., 2008c). We first studied the consequences of Scn1bb knock-down on motor axon morphology because knock-down of the a Na^+ channel α-subunit affects this phenotype. For these experiments we used the Tg(Hb9:GFP) transgenic line that expresses

GFP in motor neurons. At 72 hpf, motor axons branched more in Scn1bbMO-injected embryos than in control-injected embryos (Fig. 8 A, B; 248 ± 51 motor axon branches for Scn1bbMO vs. 171 ± 31 motor axon branches for Scn1bbCTL; p=0.0005, Student's t-test), suggesting that Scn1bb plays a role in motor axon branching in zebrafish embryos. In comparison to results obtained by knock-down of the nav1.6a α-subunit, encoded by the scn8aa gene (Pineda et al., 2006), knock-down of Scn1bb produced similar but milder motor axon phenotypes.

On the basis of the Scn1bb expression pattern, we also examined the olfactory system and inner ear for possible defects upon knock-down of Scn1bb. The olfactory nerve displayed defective morphology within the olfactory pit. In control embryos, a fasciculated olfactory nerve displayed strong acetylated α-tubulin immunoreactivity as it exited the pit and entered the bulb (Fig. 8 C). In contrast, acetylated α-tubulin immunoreactivity revealed aberrant fasciculation within the pit of morphant embryos (Fig. 8 D). Instead of the prominent fasciculated nerve evident at the point of exit from the pit, as in control embryos (Fig. 8 C, star), morphant embryos displayed several acetylated α-tubulin positive subdivisions of the nerve within the major compartment of the pit (Fig. 8 D, stars). Compared to controls, the olfactory nerve of morphants had significantly increased branches within the pit (6 +/- 2.28 for Scn1bbMO versus 1.7 +/- 0.92 for Scn1bbCTL; p=0.0001, Student's t-test). In the inner ear, there was an obvious increase in the number of hair cells in morphant embryos (Fig. 8 E, F). On average, morphant embryos had 88 +/- 13 hair cells at 72 hpf, while control embryos had only 69 +/- 19 hair cells (p=0.005).

Overall, our data support the idea that Na^+ channel β1 subunits play multiple important and diverse roles as members of ion channel complexes as well as CAMs, the latter reflecting a possible ion conduction independent function.

Discussion

In contrast to mammals, zebrafish express at least two β1 subunit genes,*scn1ba* and *scn1bb*. Our results inform about the evolutionary origins of the two zebrafish *scn1b* genes and identify potential novel roles for the newly discovered *scn1bb* gene.

Differential expression of scn1ba and scn1bb supports functional subdivision of the roles of an ancestral SCN1B gene

In mammals, a single β1 subunit gene, *SCN1B*, exists that is expressed in a cell type and developmentally specific manner (Tong et al., 1993). In contrast, zebrafish has two identified *scn1b* orthologs, *scn1ba* (Fein et al., 2007) and *scn1bb* (this study), that are located on different chromosomes. A large number of mammalian genes are represented twice in the zebrafish genome as a result of a large scale genome wide duplication event that occurred during teleost evolution (Taylor et al., 2001). Several models propose that duplicated genes were more likely to be retained throughout evolution if they underwent subfunctionalization (Lynch and Force, 2000; Lynch et al., 2001; Van de Peer et al., 2001). The differential expression patterns of *scn1ba* (principally in excitable cells) and *scn1bb* (present in excitable and non-excitable cells) supports functional subdivision of *SCN1B* function in the teleost lineage.

Shared functions of zebrafish SCN1B paralogs

Similar to Scn1ba, Scn1bb protein localizes to excitable cells (e.g., RB and other spinal cord neurons; Supplemental Fig. 2). Previous work indicated that Scn1ba plays a conventional ion channel associated function and modulates Na^+ currents (Fein et al., 2007). We found that Scn1bb also modulate Na^+ currents. However, two interesting differences exist between the electrophysiological effects of the two duplicated zebrafish genes. First, a small but significant non-inactivating Na^+ current was observed in the presence of Scn1ba, while Na^+ current inactivated completely in the presence of Scn1bb. Second, Scn1ba and Scn1bb had different

effects on the extent and rate of recovery from inactivation. These findings add further support to the view that subdivision of an ancestral *SCN1B* gene function occurred in the teleost lineage. Of the two duplicated genes, *scn1bb* is the most similar to *Scn1b* in terms of current modulation and the amino acid sequence of Scn1bb shares greater identity with Scn1b than does Scn1ba. We have proposed previously that differences in the β strands, especially the presence of proline residues, of the Ig loop domain of Scn1ba may be responsible for its different observed effects on channel modulation (Fein et al., 2007).

Novel functions of Scn1bb

In addition to excitable cells, Scn1bb protein also localizes to several different types of non-excitable cells including oligodendrocytes, Schwann cells, lateral line neuromasts, epithelial cells of the pronephros, cells of the olfactory epithelium and inner ear supporting cells. Similarly, in mammals, optic nerve astrocytes and Schwann cells express *Scn1b* (Oh and Waxman, 1994b; Oh and Waxman, 1995; Oh et al., 1997). Scn1bb distribution is reminiscent of that of the β2 subunit of Na^+/K^+ ATPase (AMOG) in excitable and non-excitable cells (Xiao et al., 1999). AMOG functions both as a CAM involved in neuron-glia interactions and as a member of the Na^+/K^+ ATPase ion transport complex (Muller-Husmann et al., 1993).

While Na^+ currents have been recorded from immature oligodendrocyte precursors in culture (Glassmeier and Jeserich, 1995; Williamson et al., 1997; Bernard et al., 2001), Na^+ currents are not detected in oligodendrocytes recorded from identified glial cells in hippocampal slices (Sontheimer and Waxman, 1993), suggesting that Na^+ channel α subunits are not expressed in mature, myelinating oligodendrocytes *in vivo.* A recent report suggests two classes of spiking and non-spiking oligodendrocyte precursor cells, due to differential expression of TTX-S Na^+ currents (Karadottir et al., 2008). Oligodendrocyte precursor cells lose Na^+ current expression as they mature, such that no currents are detected in myelinating oligodendrocytes (Sontheimer et al., 1989; Karadottir et al., 2008). Co-staining of optic nerve sections with anti-Scn1bb and pan-Na^+ channel α-subunit antibodies showed the absence of Na^+ channel α-subunits but the presence of Scn1bb in the myelin sheath. These results provide evidence that Scn1bb is expressed in the myelin in the absence of the ion-conducting pore. As discussed further below, we propose that Scn1bb functions in myelin as a CAM involved in neuron-glia interactions.

In mice, deletion of Scn1b *in vivo* results in everted paranodal loops in a subpopulation of CNS nodes of Ranvier (Chen et al., 2004), disrupted cerebellar granule neuron migration, and aberrant fasciculation of corticospinal tract axons (Brackenbury et al., 2008b). These data support a role for Scn1b in CAM complexes involved in forming septate-like junctions linking the myelin sheath to the axonal membrane, regulating growth cone migration, and mediating axonal fasciculation (Brackenbury et al., 2008a). In support of this idea, we found that knock-down of Scn1bb led to defects in the extent of branching of motor neuron axons (Fig. 8). Further, we did not detect Scn1bb protein in the motor neurons themselves but rather in Schwann cells that ensheath peripheral motor axons. These results suggest that Scn1bb influences motor axon morphology non-cell autonomously. Similarly, previous studies revealed a non-cell autonomous role for the sodium channel α subunit in regulation of motor axon development (Pineda et al., 2006).

In the olfactory epithelium, supporting cells envelop OSNs and adhere to each other via a complex that includes adherence junctions and desmosomes (Hansen and Zielinski, 2005; Hegg and Lucero, 2006). We detected Scn1bb in these supporting cells (Fig. 3 F). Knock-down of Scn1bb produced defects in the morphology of the olfactory nerve as it formed in the olfactory pit. The defasiculated appearance of the olfactory nerve in Scn1bb morphant embryos (Fig. 8) further supports a CAM role for the subunit in supporting cells of the olfactory epithelium. Inner ear supporting cells also express Scn1bb. We found that knock-down of

Scn1bb led to a ~30% increase in hair cell number (Fig. 8). Whereas the underlying mechanism is not obvious, one possibility is that lack of Scn1bb interferes with apposition of inner ear cells that is required for proper Notch signaling and specification of the appropriate number of hair cells (Kelley, 2003; Kiernan et al., 2005). Because reductions in electrical activity are not thought to be sufficient to alter neuromast patterning in the zebrafish lateral line (Grant et al., 2005), it is possible that Scn1bb-mediated cell adhesive interactions and not Scn1bb-mediated modulation of channel activity is responsible for the observed phenotype. Taken together, our findings support a CAM role for Scn1bb in supporting and epithelial cells in the absence of the Na^+ channel ion-conducting pore.

Na^+ channel β1 subunits are multi-functional

In mammals, *Scn1b* plays an essential role during development of the mammalian central nervous system *in vivo* (Brackenbury et al., 2008c). The cerebella of *Scn1b* null mice exhibit disorganized, defasciculated parallel fibers as well as abnormal cerebellar granule neuron axonal patterning through the molecular layer into the internal granule cell layer. These effects are similar to those observed in mice lacking the CAM contactin (Berglund et al., 1999). In the corticospinal tracts of *Scn1b* null mice, we observed reduced fasciculation at the pyramidal decussation, with axons projecting laterally from the dorsal column, beyond the pyramidal decussation. These effects are also consistent with disrupted CAM interactions. In the present study, we report increased axonal branching of zebrafish spinal motor neurons in the absence of Scn1bb. Further, similar to *macho, alligator*, and *steifftier* mutants, Scn1bb morphant fish have significantly reduced touch sensitivity as well as reduced Na^+ currents in RB neurons. Thus, we propose that Scn1bb serves multiple functions in the developing zebrafish nervous system: first, to regulate electrical excitability via changes in Na^+ current, and second, to modulate neuronal pathfinding through cell adhesive interactions.

Supplementary Material

Refer to Web version on PubMed Central for supplementary material.

Acknowledgements

The authors thank Drs. Matt Voas and William Talbot for their advice on whole mount immunohistochemistry techniques, Drs. Louis St.-Amant and John Kuwada for their assistance with radiation hybrid mapping, Drs. Yu-Chi Shen and Kate Barald for assistance with inner ear morphology, and Mr. Christopher Cooke for expert technical assistance. Supported by NIH MH059980 and NS51747 to LLI, by NIH F31 NS047901 to AJF, by NIH F30 NS061409 and T32 GM008497 to MAW, and by NIH NS038937 and NS048154 to ABR. AJF was also supported by the University of Michigan Pharmacological Sciences Training Program (NIH 5T32 GM007767).

References

Armstrong CM, Benzanilla F. Inactivation of the sodium channel. II. Gating current experiments. J Gen Physiol 1977;70:567–590. [PubMed: 591912]

Berglund EO, Murai KK, Fredette B, Sekerkova G, Marturano B, Weber L, Mugnaini E, Ranscht B. Ataxia and abnormal cerebellar microorganization in mice with ablated contactin gene expression. Neuron 1999;24:739–750. [PubMed: 10595523]

Bernard F, Bossu JL, Gaillard S. Identification of living oligodendrocyte developmental stages by fractal analysis of cell morphology. J Neurosci Res 2001;65:439–445. [PubMed: 11536328]

Brackenbury WJ, Isom LL. Voltage-gated Na+ channels: Potential for β subunits as therapeutic targets. Expert Opinion on Therapeutic Targets. 2008in press

Brackenbury WJ, Djamgoz MB, Isom LL. An emerging role for voltage-gated Na+ channels in cellular migration: Regulation of central nervous system development and potentiation of invasive cancers. The Neuroscientist. 2008ain press

Brackenbury WJ, Davis TH, Chen C, Slat EA, Detrow MJ, Dickendesher TL, Ranscht B, Isom LL. Voltage-gated Na+ channel beta1 subunit-mediated neurite outgrowth requires Fyn kinase and contributes to postnatal CNS development in vivo. J Neurosci 2008b;28:3246–3256. [PubMed: 18354028]

Brackenbury WJ, Davis TH, Chen C, Slat EA, Detrow MJ, Dickendesher TL, Ranscht B, Isom LL. Voltage-gated Na+ channel β1 subunt-mediated neurite outgrowth requires fyn kinase and contributes to postnatal CNS development in vivo. J Neurosci 2008c;28:3246–3256. [PubMed: 18354028]

Catterall WA. From ionic currents to molecular mechanisms: the structure and function of voltage-gated sodium channels. Neuron 2000;26:13–25. [PubMed: 10798388]

Chen C, Westenbroek RE, Xu X, Edwards CA, Sorenson DR, Chen Y, McEwen DP, O'Malley HA, Bharucha V, Meadows LS, Knudsen GA, Vilaythong A, Noebels JL, Saunders TL, Scheuer T, Shrager P, Catterall WA, Isom LL. Mice lacking sodium channel beta1 subunits display defects in neuronal excitability, sodium channel expression, and nodal architecture. J Neurosci 2004;24:4030–4042. [PubMed: 15102918]

Chopra SS, Watanabe H, Zhong TP, Roden DM. Molecular cloning and analysis of zebrafish voltage-gated sodium channel beta subunit genes: Implications for the evolution of electrical signaling in vertebrates. BMC Evol Biol 2007;7:113. [PubMed: 17623065]

Clarke JD, Hayes BP, Hunt SP, Roberts A. Sensory physiology, anatomy and immunohistochemistry of Rohon-Beard neurones in embryos of Xenopus laevis. J Physiol 1984;348:511–525. [PubMed: 6201612]

Davis TH, Chen C, Isom LL. Sodium Channel β1 Subunits Promote Neurite Outgrowth In Cerebellar Granule Neurons. J Biol Chem 2004;279:51424–51432. [PubMed: 15452131]

Diss JK, Fraser SP, Djamgoz MB. Voltage-gated Na+ channels: multiplicity of expression, plasticity, functional implications and pathophysiological aspects. Eur Biophys J 2004;33:180–193. [PubMed: 14963621]

Dolmetsch R. Excitation-transcription coupling: signaling by ion channels to the nucleus. Sci STKE 2003 2003:PE4.

Drummond I. Making a zebrafish kidney: a tale of two tubes. Trends Cell Biol 2003;13:357–365. [PubMed: 12837606]

Drummond IA. Kidney development and disease in the zebrafish. J Am Soc Nephrol 2005;16:299–304. [PubMed: 15647335]

Drummond IA, Majumdar A, Hentschel H, Elger M, Solnica-Krezel L, Schier AF, Neuhauss SC, Stemple DL, Zwartkruis F, Rangini Z, Driever W, Fishman MC. Early development of the zebrafish pronephros and analysis of mutations affecting pronephric function. Development 1998;125:4655–4667. [PubMed: 9806915]

Fashena D, Westerfield M. Secondary motoneuron axons localize DM-GRASP on their fasciculated segments. J Comp Neurol 1999;406:415–424. [PubMed: 10102505]

Fein AJ, Meadows LS, Chen C, Slat EA, Isom LL. Cloning and expression of a zebrafish SCN1B ortholog and identification of a species-specific splice variant. BMC Genomics 2007;8:226. [PubMed: 17623064]

Flanagan-Steet H, Fox MA, Meyer D, Sanes JR. Neuromuscular synapses can form in vivo by incorporation of initially aneural postsynaptic specializations. Development 2005;132:4471–4481. [PubMed: 16162647]

Girault JA, Peles E. Development of nodes of Ranvier. Current opinion in neurobiology 2002;12:476–485. [PubMed: 12367625]

Glassmeier G, Jeserich G. Changes in ion channel expression during in vitro differentiation of trout oligodendrocyte precursor cells. Glia 1995;15:83–93. [PubMed: 8847104]

Gomez-Ospina N, Tsuruta F, Barreto-Chang O, Hu L, Dolmetsch R. The C terminus of the L-type voltage-gated calcium channel Ca(V)1.2 encodes a transcription factor. Cell 2006;127:591–606. [PubMed: 17081980]

Grant KA, Raible DW, Piotrowski T. Regulation of latent sensory hair cell precursors by glia in the zebrafish lateral line. Neuron 2005;45:69–80. [PubMed: 15629703]

Hansen A, Zeiske E. Development of the olfactory organ in the zebrafish, Brachydanio rerio. J Comp Neurol 1993;333:289–300. [PubMed: 8345108]

Hansen A, Zielinski BS. Diversity in the olfactory epithelium of bony fishes: development, lamellar arrangement, sensory neuron cell types and transduction components. J Neurocytol 2005;34:183–208. [PubMed: 16841163]

Hegg CC, Lucero MT. Purinergic receptor antagonists inhibit odorant-induced heat shock protein 25 induction in mouse olfactory epithelium. Glia 2006;53:182–190. [PubMed: 16206165]

Hegle AP, Marble DD, Wilson GF. A voltage-driven switch for ion-independent signaling by ether-a-go-go K+ channels. Proc Natl Acad Sci U S A 2006;103:2886–2891. [PubMed: 16477030]

Isom LL. Sodium channel β subunits: anything but auxiliary. The Neuroscientist 2001;7:42–54. [PubMed: 11486343]

Isom LL, Catterall WA. Na^+ channel subunits and Ig domains. Nature 1996;383:307–308. [PubMed: 8848042]

Isom LL, Scheuer T, Brownstein AB, Ragsdale DS, Murphy BJ, Catterall WA. Functional co-expression of the β1 and type IIA α subunits of sodium channels in a mammalian cell line. J Biol Chem 1995;270:3306–3312. [PubMed: 7852416]

Isom LL, De Jongh KS, Patton DE, Reber BFX, Offord J, Charbonneau H, Walsh K, Goldin AL, Catterall WA. Primary structure and functional expression of the β1 subunit of the rat brain sodium channel. Science 1992;256:839–842. [PubMed: 1375395]

Johnson D, Montpetit ML, Stocker PJ, Bennett ES. The sialic acid component of the beta1 subunit modulates voltage-gated sodium channel function. J Biol Chem 2004;279:44303–44310. [PubMed: 15316006]

Kaczmarek LK. Non-conducting functions of voltage-gated ion channels. Nat Rev Neurosci 2006;7:761–771. [PubMed: 16988652]

Karadottir R, Hamilton NB, Bakiri Y, Attwell D. Spiking and nonspiking classes of oligodendrocyte precursor glia in CNS white matter. Nat Neurosci 2008;11:450–456. [PubMed: 18311136]

Kazarinova-Noyes K, Shrager P. Molecular constituents of the node of Ranvier. Mol Neurobiol 2002;26:167–182. [PubMed: 12428754]

Kazarinova-Noyes K, Malhotra JD, McEwen DP, Mattei LN, Berglund EO, Ranscht B, Levinson SR, Schachner M, Shrager P, Isom LL, Xiao Z-C. Contactin associates with Na^+ channels and increases their functional expression. J Neurosci 2001;21:7517–7525. [PubMed: 11567041]

Kelley MW. Cell adhesion molecules during inner ear and hair cell development, including notch and its ligands. Current topics in developmental biology 2003;57:321–356. [PubMed: 14674486]

Kiernan AE, Cordes R, Kopan R, Gossler A, Gridley T. The Notch ligands DLL1 and JAG2 act synergistically to regulate hair cell development in the mammalian inner ear. Development 2005;132:4353–4362. [PubMed: 16141228]

Kim DY, Mackenzie Ingano LA, Carey BW, Pettingell WP, Kovacs DM. Presenilin/gamma -secretase-mediated cleavage of the voltage-gated sodium channel beta 2 subunit regulates cell adhesion and migration. J Biol Chem. 2005

Kim DY, Carey BW, Wang H, Ingano LA, Binshtok AM, Wertz MH, Pettingell WH, He P, Lee VM, Woolf CJ, Kovacs DM. BACE1 regulates voltage-gated sodium channels and neuronal activity. Nat Cell Biol. 2007

Kohrman DC, Smith MR, Goldin AL, Harris J, Meisler MH. A missense mutation in the sodium channel Scn8a is responsible for cerebellar ataxia in the mouse mutant jolting. J Neurosci 1996;16:5993–5999. [PubMed: 8815882]

Kucenas S, Takada N, Park HC, Woodruff E, Broadie K, Appel B. CNS-derived glia ensheath peripheral nerves and mediate motor root development. Nat Neurosci 2008;11:143–151. [PubMed: 18176560]

Levitan IB. Signaling protein complexes associated with neuronal ion channels. Nat Neurosci 2006;9:305–310. [PubMed: 16498425]

Lewis KE, Eisen JS. From cells to circuits: development of the zebrafish spinal cord. Prog Neurobiol 2003;69:419–449. [PubMed: 12880634]

Lopez-Schier H, Starr CJ, Kappler JA, Kollmar R, Hudspeth AJ. Directional cell migration establishes the axes of planar polarity in the posterior lateral-line organ of the zebrafish. Dev Cell 2004;7:401–412. [PubMed: 15363414]

Lynch M, Force A. The probability of duplicate gene preservation by subfunctionalization. Genetics 2000;154:459–473. [PubMed: 10629003]

Lynch M, O'Hely M, Walsh B, Force A. The probability of preservation of a newly arisen gene duplicate. Genetics 2001;159:1789–1804. [PubMed: 11779815]

MacLean JN, Zhang Y, Johnson BR, Harris-Warrick RM. Activity-independent homeostasis in rhythmically active neurons. Neuron 2003;37:109–120. [PubMed: 12526777]

MacLean JN, Zhang Y, Goeritz ML, Casey R, Oliva R, Guckenheimer J, Harris-Warrick RM. Activity-independent coregulation of IA and Ih in rhythmically active neurons. J Neurophysiol 2005;94:3601–3617. [PubMed: 16049145]

Malhotra JD, Kazen-Gillespie K, Hortsch M, Isom LL. Sodium channel β subunits mediate homophilic cell adhesion and recruit ankyrin to points of cell-cell contact. J Biol Chem 2000;275:11383–11388. [PubMed: 10753953]

Malhotra JD, Thyagarajan V, Chen C, Isom LL. Tyrosine-phosphorylated and nonphosphorylated sodium channel beta1 subunits are differentially localized in cardiac myocytes. J Biol Chem 2004;279:40748–40754. [PubMed: 15272007]

Malhotra JD, Koopmann MC, Kazen-Gillespie KA, Fettman N, Hortsch M, Isom LL. Structural requirements for interaction of sodium channel β1 subunits with ankyrin. J Biol Chem 2002;277:26681–26688. [PubMed: 11997395]

McCormick KA, Isom LL, Ragsdale D, Smith D, Scheuer T, Catterall WA. Molecular determinants of Na^+ channel function in the extracellular domain of the β1 subunit. J Biol Chem 1998;273:3954–3962. [PubMed: 9461582]

McEwen DP, Isom LL. Heterophilic interactions of sodium channel beta 1 subunits with axonal and glial cell adhesion molecules. J Biol Chem 2004;279:52744–52752. [PubMed: 15466474]

McEwen DP, Meadows LS, Chen C, Thyagarajan V, Isom LL. Sodium channel β1 subunit-mediated modulation of Nav1.2 currents and cell surface density is dependent on interactions with contactin and ankyrin. J Biol Chem 2004;279:16044–16049. [PubMed: 14761957]

McPhee JC, Ragsdale DS, Scheuer T, Catterall WA. A critical role for transmembrane segment IVS6 of the sodium channel alpha subunit in fast inactivation. J Biol Chem 1995;270:12025–12034. [PubMed: 7744852]

Muller-Husmann G, Gloor S, Schachner M. Functional characterization of beta isoforms of murine Na,K-ATPase. The adhesion molecule on glia (AMOG/beta 2), but not beta 1, promotes neurite outgrowth. J Biol Chem 1993;268:26260–26267. [PubMed: 7504672]

Nicolson T. The genetics of hearing and balance in zebrafish. Annu Rev Genet 2005;39:9–22. [PubMed: 16285850]

Novak AE, Taylor AD, Pineda RH, Lasda EL, Wright MA, Ribera AB. Embryonic and larval expression of zebrafish voltage-gated sodium channel alpha-subunit genes. Dev Dyn 2006;235:1962–1973. [PubMed: 16615064]

Oh Y, Waxman SG. The beta 1 subunit mRNA of the rat brain Na+ channel is expressed in glial cells. Proc Natl Acad Sci U S A 1994a;91:9985–9989. [PubMed: 7937931]

Oh Y, Waxman SG. The β1 subunit mRNA of the rat brain Na^+ channel is expressed in glial cells. Proc Natl Acad Sci USA 1994b;91:9985–9989. [PubMed: 7937931]

Oh Y, Waxman SG. Differential Na+ channel beta 1 subunit mRNA expression in stellate and flat astrocytes cultured from rat cortex and cerebellum: a combined in situ hybridization and immunocytochemistry study. Glia 1995;13:166–173. [PubMed: 7782102]

Oh Y, Lee YJ, Waxman SG. Regulation of Na^+ channel β1 and β2 subunit mRNA levels in cultured rat astrocytes. Neuroscience letters 1997;234:107–110. [PubMed: 9364509]

Pineda RH, Heiser RA, Ribera AB. Developmental, molecular, and genetic dissection of INa in vivo in embryonic zebrafish sensory neurons. J Neurophysiol 2005;93:3582–3593. [PubMed: 15673553]

Pineda RH, Svoboda KR, Wright MA, Taylor AD, Novak AE, Gamse JT, Eisen JS, Ribera AB. Knockdown of Nav1.6a Na+ channels affects zebrafish motoneuron development. Development 2006;133:3827–3836. [PubMed: 16943272]

Postlethwait JH. The zebrafish genome in context: ohnologs gone missing. J Exp Zoolog B Mol Dev Evol. 2006

Raible DW, Kruse GJ. Organization of the lateral line system in embryonic zebrafish. J Comp Neurol 2000;421:189–198. [PubMed: 10813781]

Ribera AB, Nüsslein-Volhard C. Zebrafish touch-insensitive mutants reveal an essential role for the developmental regulation of sodium currents. J Neurosci 1998;18:9181–9191. [PubMed: 9801358]

Sapede D, Gompel N, Dambly-Chaudiere C, Ghysen A. Cell migration in the postembryonic development of the fish lateral line. Development 2002;129:605–615. [PubMed: 11830562]

Shapiro L, Doyle JP, Hansley P, Colman DR, Hendrikson WA. Crystal structure of the extracellular domain from P_0, the major structural protein of peripheral nerve myelin. Neuron 1996;17:435–449. [PubMed: 8816707]

Sontheimer H, Waxman SG. Expression of voltage-activated ion channels by astrocytes and oligodendrocytes in the hippocampal slice. J Neurophysiol 1993;70:1863–1873. [PubMed: 7507520]

Sontheimer H, Trotter J, Schachner M, Kettenmann H. Channel expression correlates with differentiation stage during the development of oligodendrocytes from their precursor cells in culture. Neuron 1989;2:1135–1145. [PubMed: 2560386]

Srinivasan J, Schachner M, Catterall WA. Interaction of voltage-gated sodium channels with the extracellular matrix molecules tenascin-C and tenascin-R. Proc Natl Acad Sci U S A 1998;95:15753–15757. [PubMed: 9861042]

Taylor JS, Van de Peer Y, Braasch I, Meyer A. Comparative genomics provides evidence for an ancient genome duplication event in fish. Philos Trans R Soc Lond B Biol Sci 2001;356:1661–1679. [PubMed: 11604130]

Tong J, Potts JF, Rochelle JM, Seldin MF, Agnew WS. A Single ß1 Subunit Mapped to Mouse Chromosome 7 may be a Common Component of Na Channel Isoforms from Brain, Skeletal, Muscle and Heart. Biochem Biophys Res Comm 1993;195:679–685. [PubMed: 7690558]

Tsujikawa M, Malicki J. Intraflagellar transport genes are essential for differentiation and survival of vertebrate sensory neurons. Neuron 2004;42:703–716. [PubMed: 15182712]

Van de Peer Y, Taylor JS, Braasch I, Meyer A. The ghost of selection past: rates of evolution and functional divergence of anciently duplicated genes. J Mol Evol 2001;53:436–446. [PubMed: 11675603]

Voas MG, Lyons DA, Naylor SG, Arana N, Rasband MA, Talbot WS. alpha II-Spectrin is essential for assembly of the nodes of Ranvier in myelinated axons. Current Biology. 2007in press

Westerfield, M. The Zebrafish Book: a guide for the laboratory use of zebrafish (Brachydanio rerio). University of Oregon Press; Eugene, OR: 1995.

Whitfield TT. Lateral line: precocious phenotypes and planar polarity. Curr Biol 2005;15:R67–70. [PubMed: 15668161]

Williamson AV, Compston DA, Randall AD. Analysis of the ion channel complement of the rat oligodendrocyte progenitor in a commonly studied in vitro preparation. Eur J Neurosci 1997;9:706–720. [PubMed: 9153577]

Wong HK, Sakurai T, Oyama F, Kaneko K, Wada K, Miyazaki H, Kurosawa M, De Strooper B, Saftig P, Nukina N. beta subunits of voltage-gated sodium channels are novel substrates of BACE1 and gamma -secretase. J Biol Chem. 2005

Woods IG, Lyons DA, Voas MG, Pogoda HM, Talbot WS. nsf is essential for organization of myelinated axons in zebrafish. Curr Biol 2006;16:636–648. [PubMed: 16581508]

Woods IG, Wilson C, Friedlander B, Chang P, Reyes DK, Nix R, Kelly PD, Chu F, Postlethwait JH, Talbot WS. The zebrafish gene map defines ancestral vertebrate chromosomes. Genome research 2005;15:1307–1314. [PubMed: 16109975]

Xiao Z-C, Ragsdale DS, Malhorta JD, Mattei LN, Braun PE, Schachner M, Isom LL. Tenascin-R is a functional modulator of sodium channel β subunits. J Biol Chem 1999;274:26511–26517. [PubMed: 10473612]

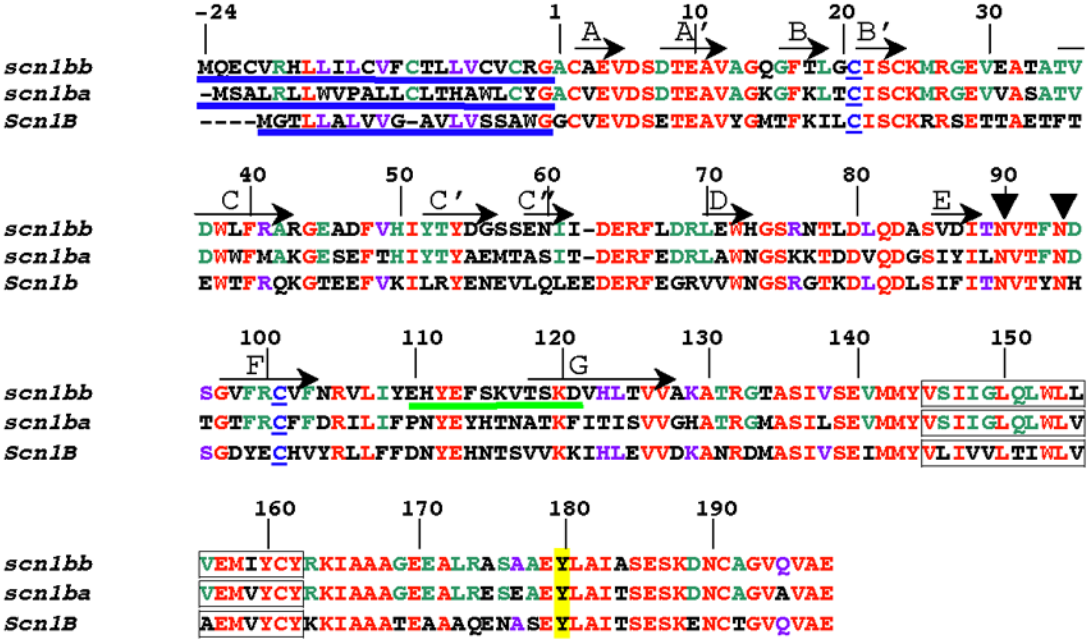

Figure 1. Alignment of Scn1bb, Scn1ba_tv1, and Scn1b

Numbering of the amino acid residues in this figure corresponds to Scn1bb. Shown in red are the residues that are identical between Scn1bb, Scn1ba, and Scn1b. Residues in purple are residues that are shared by Scn1bb and Scn1b but not shared with Scn1ba. (Scn1ba comprises two different splice variants, Scn1ba_tv1 and Scn1ba_tv2. For purposes of clarity, we have shown the sequence for only one of the two splice variants, Scn1ba_tv1). Residues in green are conserved within the two fish paralogs, but not shared with Scn1b. N-terminal signal peptides are underlined in blue. Also indicated in blue are the two cysteine residues in each subunit that are predicted to form the Ig loop domain. Predicted β-sheets in the Ig loop domain, based on the crystal structure of myelin P_0 (Shapiro et al., 1996), are indicated by arrows and labeled with capital letters (A through G). Predicted glycosylation sites at asparagine residues in Scn1bb are indicated by τ at N-90 and N-94. These sites were determined using NetNGlyc 1.0 (http://www.cbs.dtu.dk). Predicted transmembrane spanning segments are indicated as boxed residues. The tyrosine residue, Y-180, homologous to Y-181 in Scn1b (Malhotra et al., 2004), is highlighted in yellow. The peptide sequence used for anti-Scn1bb antibody production is underlined in green.

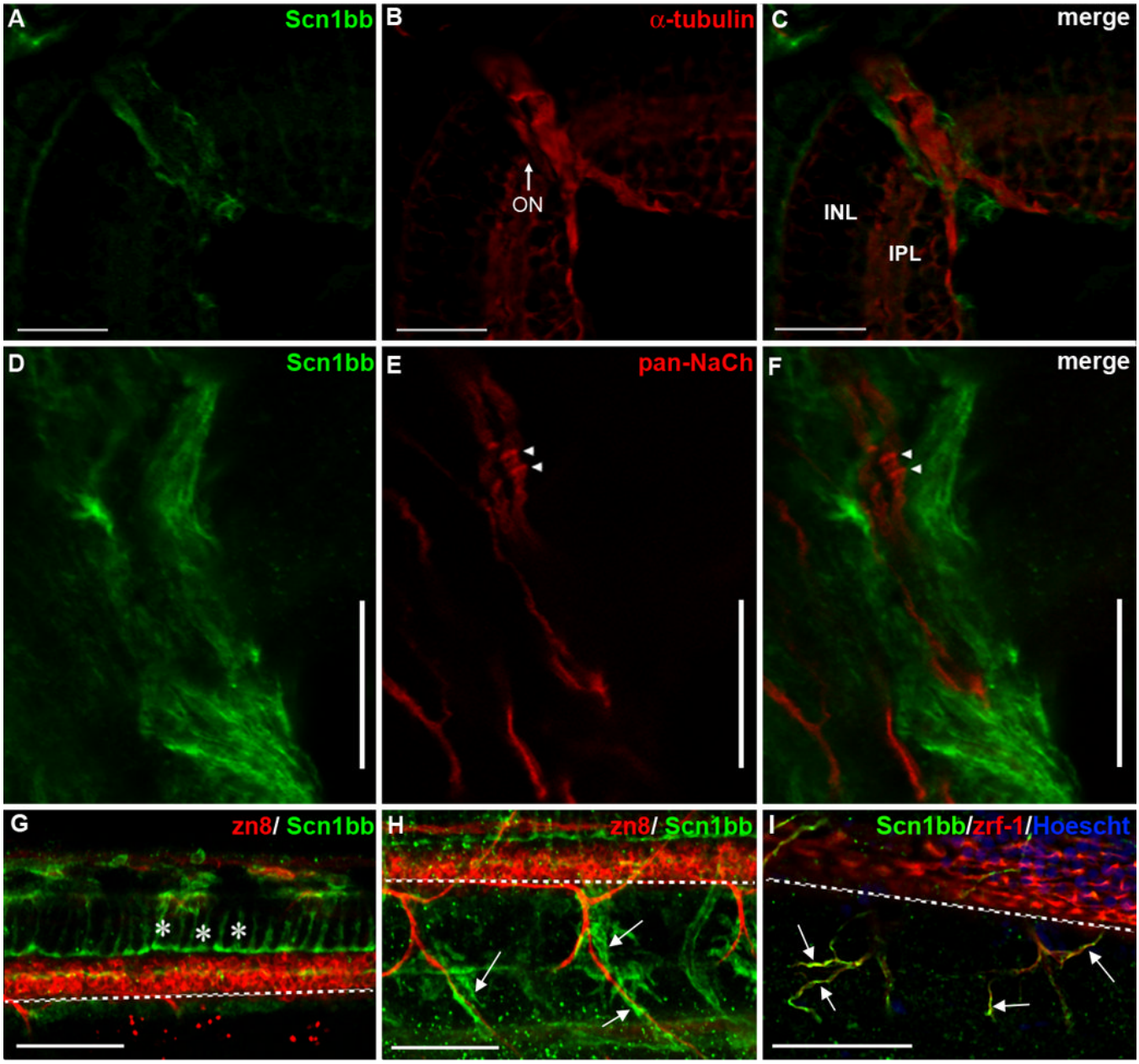

Figure 2. Scn1bb is expressed in optic nerve and spinal cord glia

A - C: Cryosections; scale bars, 25 μm. A. At 5 dpf, the retina displays little or no Scn1bb immunoreactivity (green). However, cells surrounding the optic nerve (ON) are strongly Scn1bb immunopositive. B. Acetylated α-tubulin (red) staining is observed in layers of the retina (e.g., inner plexiform layer, IPL) and strongly labels the optic nerve (ON). C. The merged image of Panels A and B demonstrates that Scn1bb (green) and acetylated α-tubulin (red) immunoreactivites do not overlap in the optic nerve. In addition, the Scn1bb signal surrounds that of the neuronal marker acetylated α-tubulin, indicating that Scn1bb immunopositive cells localize to the location of optic nerve myelin. D - F: Dissected optic nerves; scale bars, 10 μm. D. We detected strong Scn1bb immunoreactivity in optic nerves dissected from adult zebrafish. E. In addition to Scn1bb, isolated adult optic nerves display axonal expression of pan-Na^+ channel α-subunits (NaCh, red). Na^+ channel α-subunit clusters, possibly hemi-nodes,

are indicated with arrowheads. F. The merged image shows that Scn1bb (green) and Na^+ channel α-subunit (red) immunoreactivities are non-overlapping, consistent with Scn1bb expression in the myelinating glia that ensheath the retinal ganglion cell axons within the optic nerve. G-I: Lateral view of whole mount 72 hpf embryos, anterior to the left, dorsal at the top; Scale Bars, 50um. The dashed white line indicates the ventral boundary of the spinal cord. G. Radial glia (asterisks) in the spinal cord express Scn1bb (green) and can be identified by their characteristic elongated morphology, stretching from the dorsal spinal cord to just above the secondary motor neurons (labeled with zn8, red). H. Scn1bb-positive cells (green, arrows) surround, but do not overlap with, ventral motor neuron axons (labeled with zn8, red). I. Scn1bb (green) co-localizes with the Schwann cell marker zrf-1 (red), suggesting Scn1bb is expressed in Schwann cells (arrows) that ensheath peripheral motor axons.

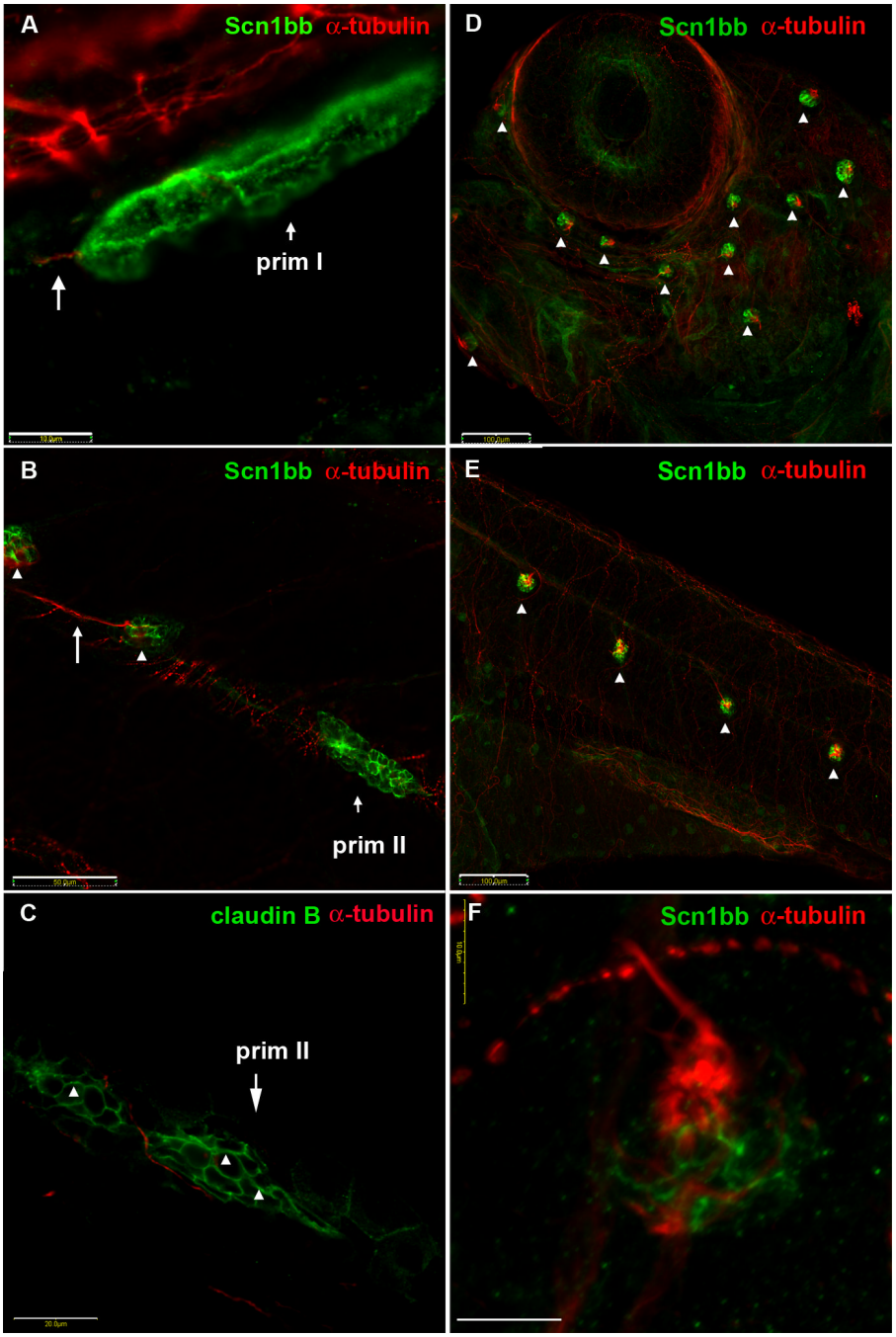

Figure 3. Scn1bb is expressed in migrating primordia and neuromasts of the lateral line system

A-C: Migrating primordia and newly formed neuromasts express Schn1bb protein. A. Immunocytochemistry reveals non-overlapping expression of both Scn1bb (green) and acetylated α-tubulin (red) proteins in the migrating prim I lateral line primordium of 28 hpf embryos. The octavolateralis system axons (long arrow), that trail prim I, display acetylated α-tubulin immunoreactivity. Scale bar, 10 μm. B. In 5 dpf larvae, the prim II lateral line primordium and newly deposited neuromasts express Scn1bb (green). However, prim II (short arrow) and newly deposited neuromasts (arrow heads) do not express acetylated α-tubulin. In contrast, an innervating neurite (long arrow) is positive for acetylated α-tubulin immunoreactivity. Scale Bar, 50 μm. C. Similar to Scn1bb, claudin b (arrow heads) is present

in prim II in a complementary pattern to anti-acetylated α-tubulin. Scale Bar, 50 μm. D - F: ALL and PLL neuromasts express Scn1bb protein. D. In 5 dpf embryos, anti-Scn1bb (green) specifically reveals neuromasts of the ALL (arrowheads). Scn1bb and acetylated α-tubulin (red) are expressed in different domains of the ALL neuromasts. Anti-acetylated α-tubulin marks the kinocilia of ALL neuromasts. Scale Bar, 100 μm. E. In 5 dpf embryos, anti-Scn1bb (green) also is present within the neuromasts of the PLL (arrow heads). Similar to the ALL, Scn1bb and acetylated α-tubulin (red) are expressed in different domains of the PLL neuromasts. Scale Bar, 100 μm. F. Different cell types within a neuromast express Scn1bb (green) and acetylated α-tubulin (red). Supporting cells display Scn1bb immunoreactivity, whereas hair cells express acetylated α-tubulin (red) in the soma and projecting kinocilia. Scale Bar, 10 μm.

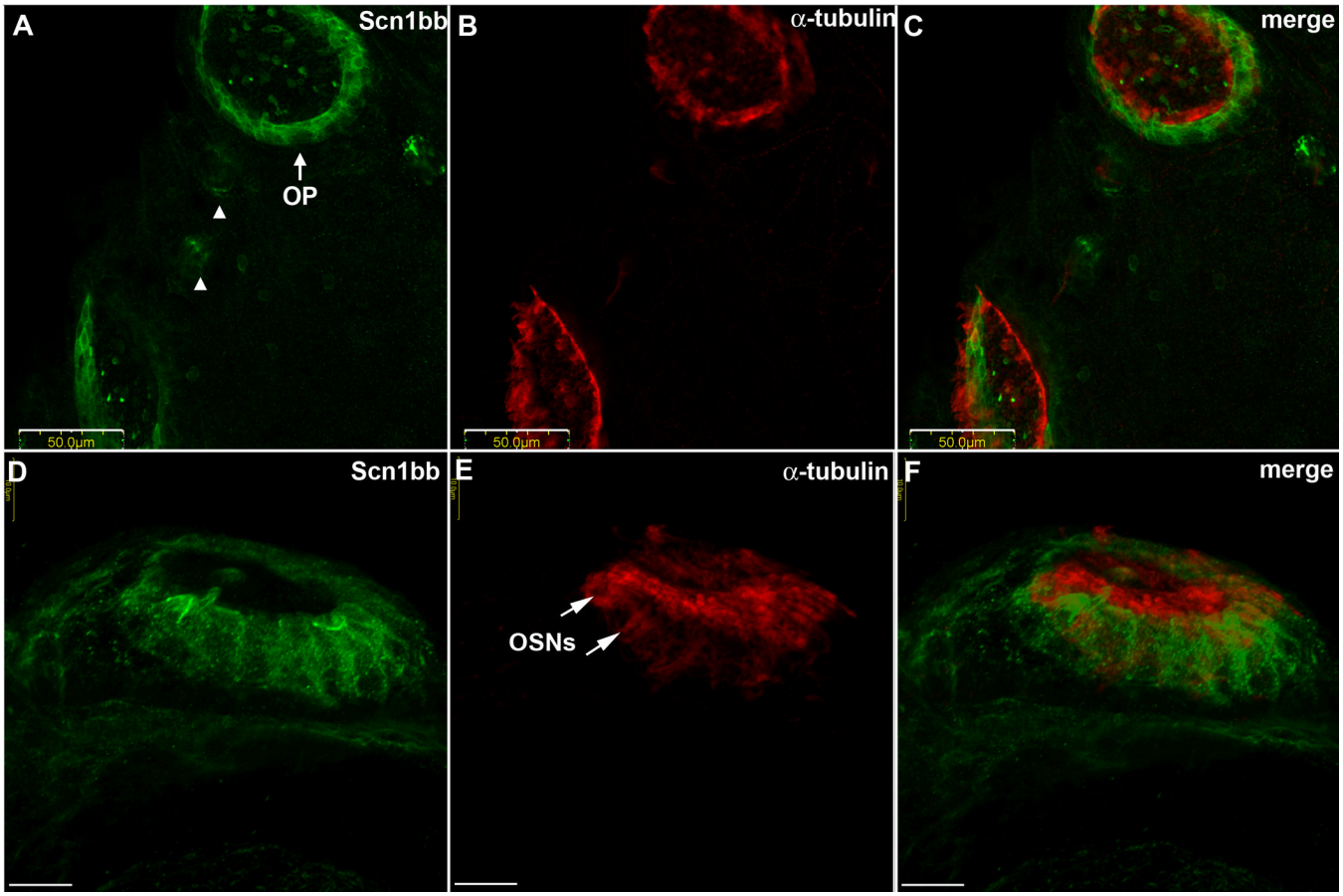

Figure 4. Scn1bb is expressed in the supporting cell bodies of the olfactory pits

A. Anti-Scn1bb (green) labels a ring of cell bodies in the olfactory pits (OP) and the intervening neuromasts (arrowheads) in fish that are 5 dpf. B. Anti-acetylated α-tubulin (red) labels olfactory pits in a ring corresponding to cilia and kinocilia. C. Merged image showing that anti-Scn1bb (green) and anti-acetylated α-tubulin (red) staining are non-overlapping. D. High magnification image of a side view of an olfactory pit shows Scn1bb (green) expression in the supporting cell bodies. E. Anti-acetylated α-tubulin (red) stains the layer of kinocilia projecting from supporting cells and ciliated OSN dendritic knobs (arrows). F. Non-overlapping expression of Scn1bb (green) in the supporting cell bodies and acetylated α-tubulin (red) in the kinocilia, cilia, and OSN dendritic knobs. Scale Bars, A - C: 50 μm; D - F: 10 μm.

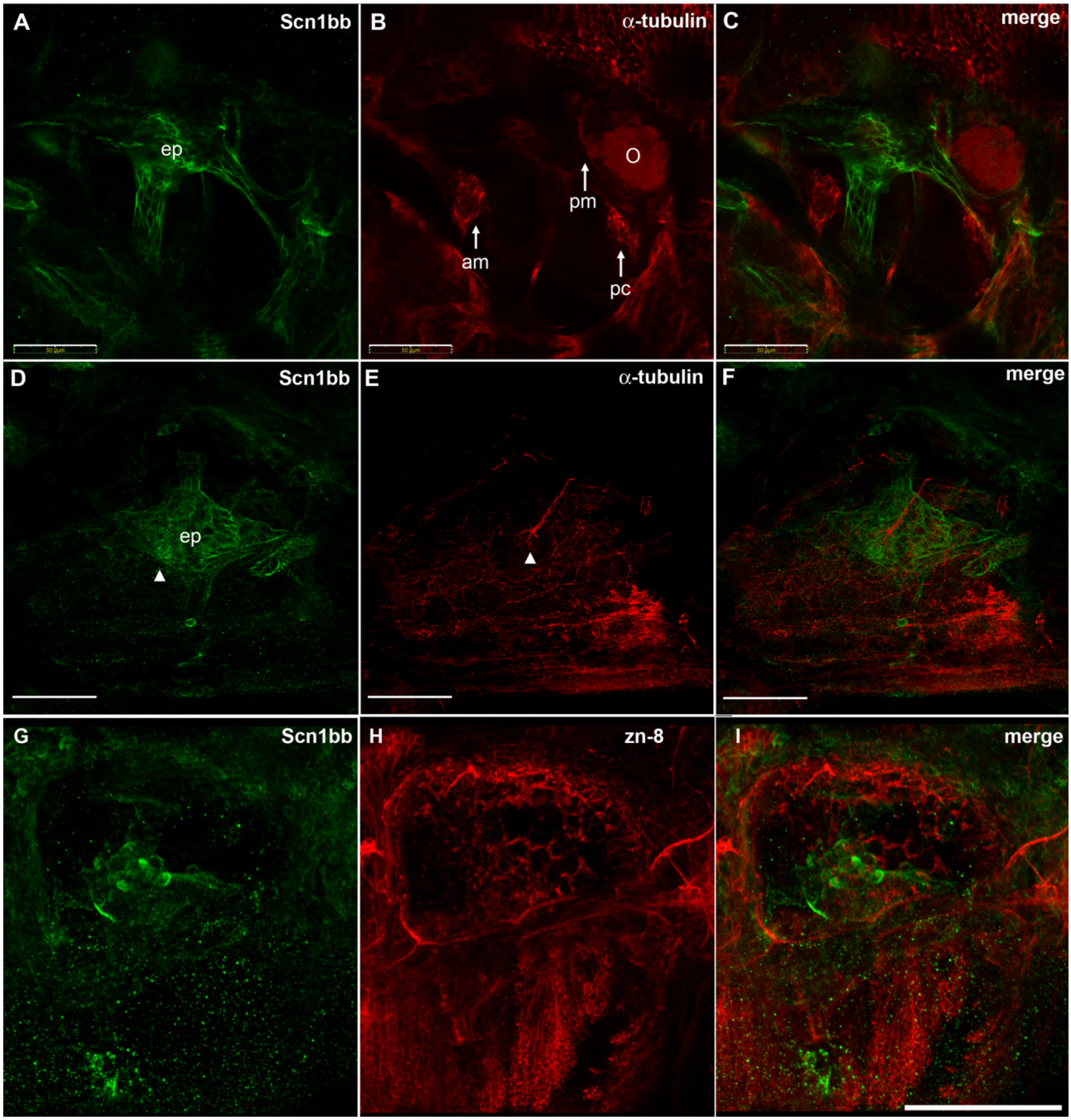

Figure 5. Scn1bb is expressed in the semi-circular canals of the inner ear

A. Anti-Scn1bb (green) labels the epithelial pillars (ep) of the semi-circular canal in 5 dpf fish. B. Anti-acetylated α-tubulin (red) labels the sensory patches found in inner ear (O, otolith; am, anterior macula; pc, posterior crista; pm, posterior macula). C. Merged image shows that expression of Scn1bb (green) and acetylated α-tubulin (red) is non-overlapping. D. Anti-Scn1bb labels the base of the otic neuromast (arrowhead) in addition to the epithelial pillars. E. Anti-acetylated α-tubulin labels the kinocilia projecting from the otic neuromast (arrowhead). F. The two expression domains are non-overlapping. G. Anti-Scn1bb (green) labels the otic vesicle in 72 hpf fish. H. Zn-8 (red). I. Merged image. Scale Bars, A - F: 50 μm: G - I: 100 μm.

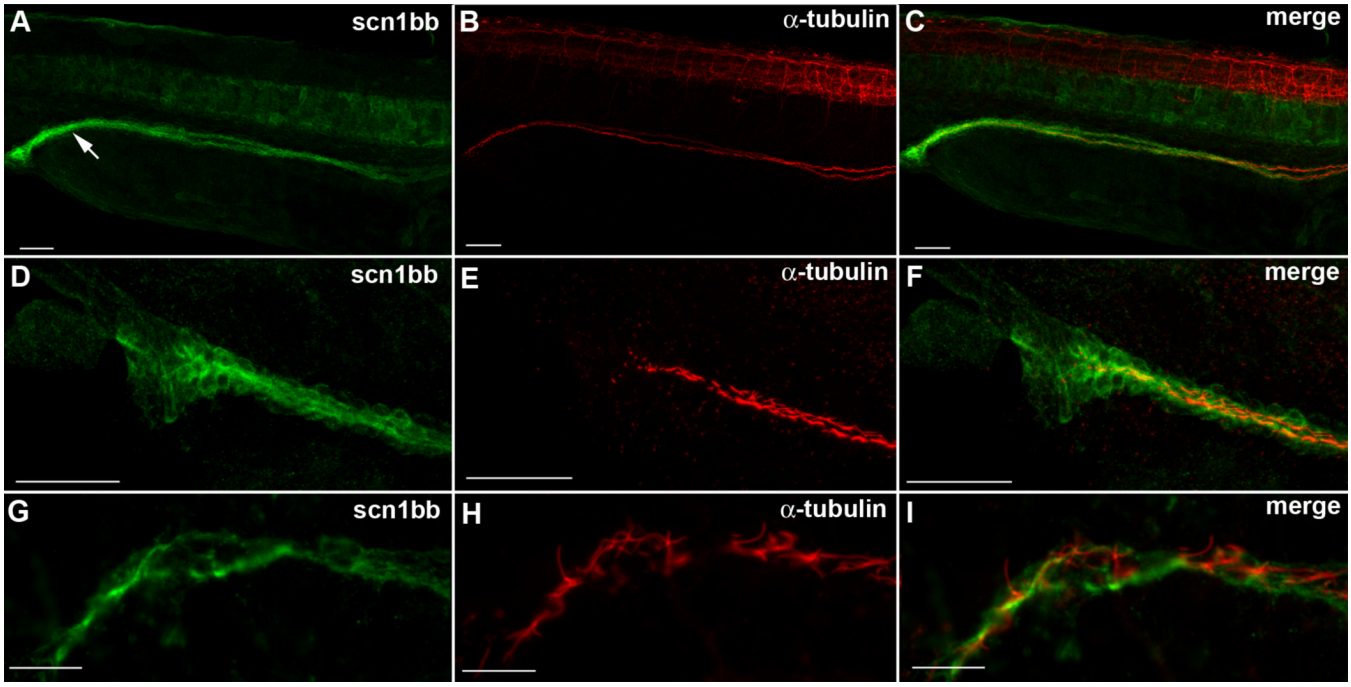

Figure 6. Scn1bb is expressed in the epithelial cells of the pronephric duct

A. Anti-Scn1bb (green) labeled the cells spanning the pronephric duct (arrow) in 28 hpf fish. B. Anti-acetylated α-tubulin (red) labeled the cilia that line the pronephric duct. C. Anti-Scn1bb (green) and anti-acetylated α-tubulin (red) co-labeled the pronephric duct. D. Anti-Scn1bb (green) labeled epithelial cells of the pronephric duct. E. Anti-acetylated α-tubulin (red) labeled the ciliated interior of the pronephric duct. F. Expression of scn1bb (green) and acetylated α-tubulin (red) is non-overlapping. G. High magnification image of anti-Scn1bb positive (green) epithelial cells. H. High magnification image of anti-acetylated α-tubulin positive (red) cilia. I. Merged image with expression of Scn1bb (green) and acetylated α-tubulin (red) non overlapping. Scale Bars, A - F: 50 μm; G - I: 10 μm.

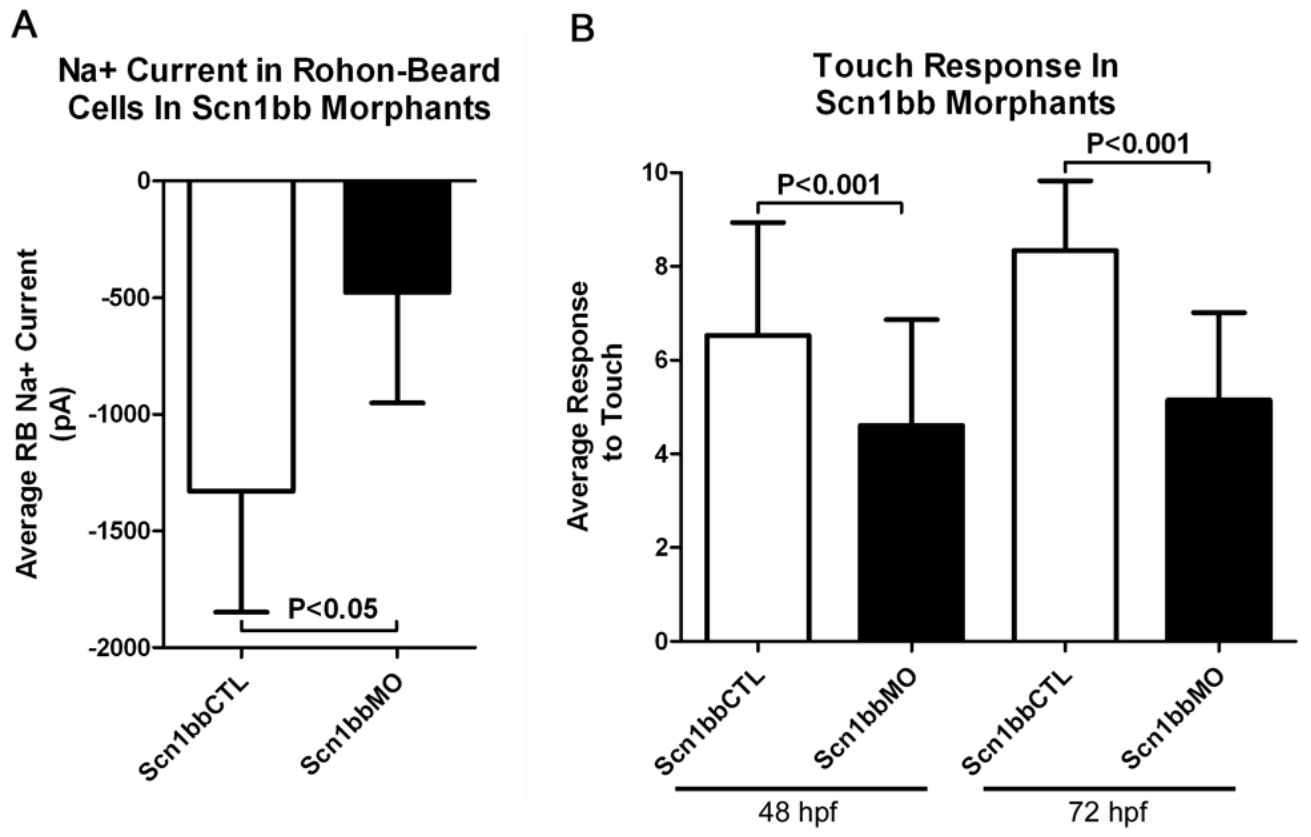

Figure 7. Embryos injected with Scn1bbMO have reduced Na^+ current amplitudes in RB neurons and display touch insensitivity

A. Peak Na^+ current in RB neurons average -1329.5 +/- 518.7 pA in embryos injected with Scn1bbCTL (n=4), but only -477.2 +/- 474.7 in embryos injected with Scn1bbMO (n=5; $p<0.05$; Student's t-test). B. At 48 hpf, embryos injected with Scn1bbMO had an average response to touch of 4.6 +/- 2.3 (n=180), compared to an average response of 6.5 +/- 2.4 (n=180) in embryos injected with Scn1bbCTL ($p<0.001$; ANOVA). Similarly, 72 hpf embryos injected with Scn1bb had an average response to touch of 5.1 +/- 1.9 (n=163) compared with an average response of 8.3 +/- 1.5 (n=60) in embryos injected with Scn1bbCTL ($p<0.001$; ANOVA).

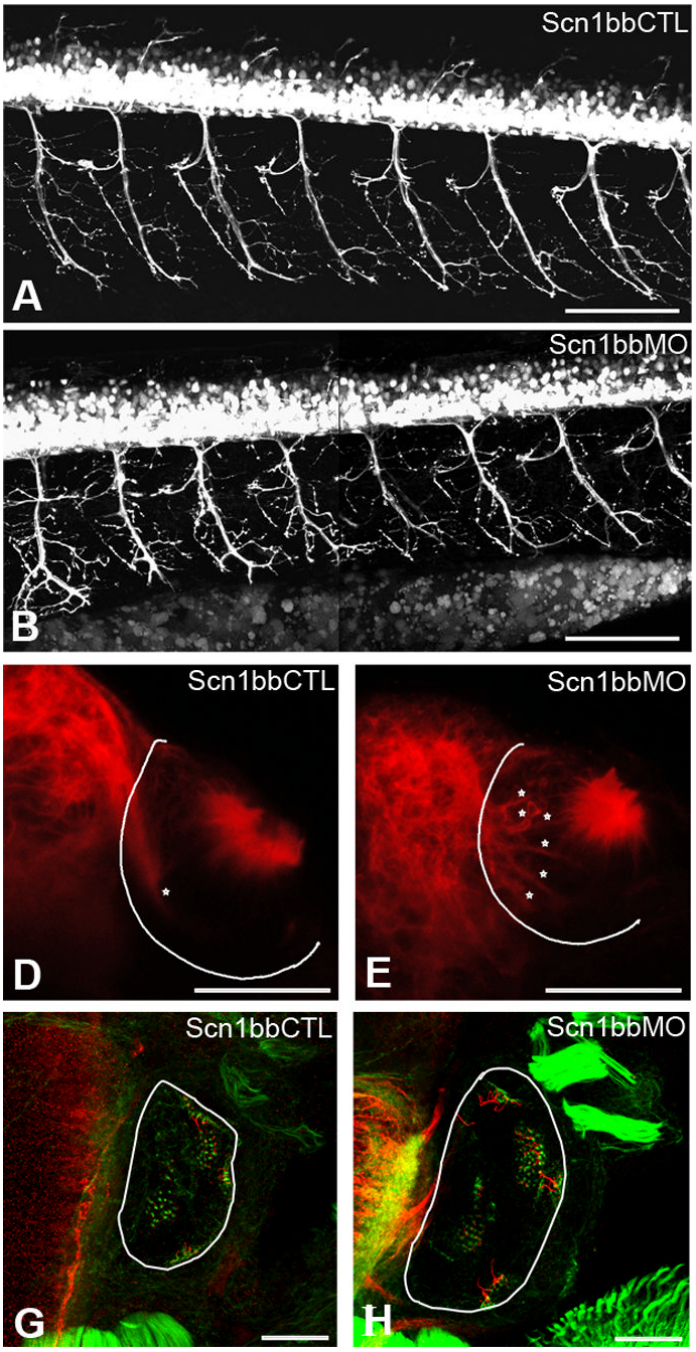

Figure 8. Scn1bbMO leads to abnormal development of motor axons, the olfactory nerve, and hair cells

A, B: Lateral views of live 72 hpf Tg(Hb9:GFP) embryos injected with Scn1bbCTL (A) or Scn1bbMO (B); anterior is to the left, and dorsal is at the top. Scale Bar, 100 μm. C, D: Abnormal fasciculation of the olfactory nerve (stars) within the olfactory pit (outlined in white) in 72 hpf embryos injected with Scn1bbMO (D) versus Scn1bbCTL (C). The olfactory nerve is visualized with an immunostain against α-acetylated tubulin (red). Scale Bar, 50 μm. E, F: Hair cells within the otic vesicle (outlined in white) of 72 hpf embryos injected with Scn1bbCTL (E) or Scn1bbMO (F) visualized with phalloidin (green) and alpha acetylated tubulin (red). Scale Bar, 50 μm.